PREDICTION OF R-CURVES FROM SMALL COUPON TESTS

J.R. Yeh, G.H. Bray, R.J. Bucci
Aluminum Company of America
Alcoa Center, PA 15069

Y. Macheret*

SUMMARY

R-curves were predicted for Alclad 2024-T3 and C188-T3 sheet using the results of small-coupon Kahn tear tests in combination with two-dimensional elastic-plastic finite element stress analyses. The predictions were compared to experimental R-curves from 6.3, 16 and 60-inch wide M(T) specimens and good agreement was obtained. The method is an inexpensive alternative to wide panel testing for characterizing the fracture toughness of damage-tolerant sheet alloys. The usefulness of this approach was demonstrated by performing residual strength calculations for a two-bay crack in a representative fuselage structure. C188-T3 was predicted to have a 24% higher load carrying capability than 2024-T3 in this application as a result of its superior fracture toughness.

INTRODUCTION

The R-curve approach to fracture toughness evaluation can be advantageously applied to thin, ductile materials where slow, stable tearing is likely to precede rapid fracture. The R-curve portrays toughness development, or resistance to crack extension, as a crack extends under continuously increasing applied load or displacement. In thin, ductile materials, the toughness increases with crack extension until a plateau is reached beyond which the toughness remains essentially constant. The R-curve is a function of material and thickness and is essentially independent of planar geometry within reasonably broad limits. These are very important attributes because they enable residual strength predictions to be made for complex structural configurations using R-curve data from much simpler test specimen geometries.

R-curves for sheet products are typically obtained from center-cracked M(T) panels. For tough sheet materials like 2024-T3, panel widths in excess of 48 inches are required to obtain the complete R-curve measurement (i.e., up to the plateau). Testing this size specimen is often not feasible due to limited material quantities, test machine and setup limitations, or high cost. For this reason, tests on small M(T) panels or toughness indicator tests such as Kahn tear or notched tensile are often used to characterize toughness. These tests are inexpensive and require only small amounts of material. However, the fracture toughness data obtained are geometry dependent, provide only relative rankings of fracture toughness, and may be of little or no use for predicting fracture behavior and residual strength in actual structures.

Thus, there is a need to develop methods to predict structural component performance from small test-coupon data. One such method developed at the Alcoa Technical Center allows a complete R-curve to be predicted from results of a Kahn tear test (ref. 1). This method has the advantages of a

---

* Formerly at Aluminum Company of America, Alcoa Center, PA.

small-coupon indicator test while preserving the true property measurement capabilities of wide-panel R-curve tests.

The prediction method is based on two fracture parameters derived from a Kahn tear test record using finite element analysis: the J-integral for crack initiation, J_i, and the critical crack-tip opening area for propagation for a given distance behind the crack tip, A_p (Figure 1). The latter criterion assumes that the area under the crack profile near to the crack tip is constant during crack extension. J_i is assumed to control crack initiation and A_p is assumed to control crack extension. The crack-tip opening area criterion is similar to a crack tip opening angle (CTOA) criterion which has been the subject of several recent studies (refs. 2 and 3). These studies indicate that CTOA is nearly constant after a small amount of crack growth . Newman et al. (ref. 4) used the CTOA criteria in combination with finite element analysis to predict the load-load line displacement response for various M(T) panels, and found good agreement between the predictions and test data.

A_p was selected over CTOA or CTOD in the current method because it proved less sensitive to changes in finite element mesh size. This is illustrated schematically in Figure 2 which shows a critical crack profile plotted after crack extensions to **a** and **b** during crack propagation. The element size behind the crack tip at **a** is half that at **b**. By fitting the critical crack-tip opening area at crack tip **a,** the critical line **b-e** is predicted at crack tip **b**. Similarly, CTOA(α_c) and CTOD (δ_c) from crack tip **a** yield critical lines **b-d** and **b-f,** respectively. It can be seen that applying the CTOD criterion from one element size to a larger element size under predicts the critical line, while the CTOA criterion overpredicts the critical line. The A_p criterion enables the element size to be changed along the line of crack extension and for different panel sizes while the CTOA and CTOD criteria require an absolute element size and arrangement along the line of crack extension and for every panel size. The ability to change element size becomes important for large panel predictions since it is very computer time consuming to make wide panel predictions using the same element size as for the small Kahn tear specimen.

In the current study, the method was applied to predict the R-curves of two damage-tolerant aluminum sheet alloys: 2024-T3 and C188-T3. C188 is a new alloy with improved toughness and fatigue crack growth resistance intended to replace 2024 in aircraft skin sheet applications. The predicted and experimentally-obtained R-curves were used to make residual strength predictions for a two-bay crack in a representative fuselage structure.

EXPERIMENTAL PROCEDURES

Materials and Mechanical Testing

Alclad 2024-T3 and C188-T3 sheet with a nominal thickness of 0.063 inch were obtained from NASA and Boeing Commercial Airplane Group, respectively. The panels were remnants of 60-inch wide M(T) specimens previously tested at Boeing. The load-COD curves from these tests were also provided by Boeing. Both materials were produced by Alcoa and were of recent vintage.

A single tensile specimen in the L direction was tested from each material in accordance with ASTM E8. The specimens were standard sheet type with a gage length of 2 inches and a uniform gage width of 0.5 inch. The extensometer remained on the specimen to failure to obtain the full stress-strain curve.

Duplicate Kahn tear specimens (Figure 3) in the L-T orientation were tested from each material using standard practices in place at the Alcoa Technical Center (ref. 5). The specimens were pulled to

failure at a crosshead speed of 0.1 inch/min. Load versus load-line displacement was acquired digitally by computer.

R-curve tests on M(T) specimens in the L-T orientation were performed in accordance with ASTM E561. A single 6.3-inch wide specimen was tested for 2024-T3 and single 6.3 and 16-inch specimens for C188-T3. The specimens were fatigue precracked at R=0.1 at a maximum net section stress of 25 to 35% of the yield strength. The precrack was extended approximately 0.125" from each side of the machined slot to an initial crack length $2a_o$ of approximately 0.25 the panel width, W. After precracking, anti-buckling restraints composed of rigid face plates were attached to the specimen. The specimens were pulled to failure under displacement control. The displacement rate was approximately 0.3 inch/min. for the 2024-T3 specimen and 0.1 inch/min. for the C188-T3 specimens. Load versus crack opening displacement (COD) was acquired digitally by computer. R-curves were calculated from the load-COD curves using the secant compliance method of ASTM E561. R-curves were also determined by this same method for the 60-inch wide specimens from the load-COD curves provided by Boeing.

Prediction of R-Curves

R-curves for 6.3, 16 and 60-inch wide M(T) specimens were predicted for C188-T3 and 2024-T3 using a method developed at Alcoa Technical Center (ref. 1). The first step in the method is to obtain the J-integral for crack initiation, J_i, and the critical crack-tip opening area for propagation area, A_p, from the Kahn tear test results. The true stress-strain curve and initial estimates of J_i and A_p are input into a 2-D finite element model of the Kahn tear specimen (Figure 3). Because of symmetry, only half the specimen is considered. A displacement is imposed on the model at the loading pin and nodes in the model along the line of crack extension are disconnected to simulate crack growth. The first node is released when the J-integral at the notch tip exceeds the initial estimate of J_i. Subsequent nodes are released when the crack-tip opening area exceeds the initial estimate of A_p. J_i and A_p are adjusted iteratively to obtain the best possible agreement between the model response and the experimental response of the Kahn tear test specimen. The force on the first node at release, F, is also noted after the final values of J_i and A_p are obtained.

The values of J_i and A_p obtained by fitting the Kahn tear test specimen response are subsequently input into a 2-D finite element model of an M(T) specimen (Figure 4). In this case, only one quarter of the specimen is considered because of symmetry. A uniform displacement is imposed on the top edge of the model. Crack extension is simulated by releasing the first node when the J-integral exceeds J_i. The finite element mesh size for the first few nodes is identical to that in the Kahn tear model. However, it is found that the force on the first node at release, F, depends on panel width and differs from that in the Kahn tear simulation. The assumption is made that the product of the force at node release and the critical crack-tip opening area is constant (i.e., geometry independent), and the critical crack-tip opening area, A_p, for the M(T) panel is determined from the relationship:

$$(F^*A_p)_{\text{Kahn tear}} = (F^*A_p)_{\text{M(T)}} \qquad (1)$$

Subsequent nodes are released when the crack opening area exceeds the calculated A_p for the M(T) specimen. The mesh size is increased after the first few nodes in order to reduce computation time. The load-COD curve predicted by this procedure is analyzed using the secant compliance method of ASTM E561 to obtain the predicted R-curve.

The need to adjust A_p using Equation 1 is not completely understand at this time. Without this adjustment (i.e., A_p held constant), the applied load is consistently over predicted by the method and

the magnitude of this over prediction increases with increasing panel size. One possibility is that the experimental loads are reduced by panel buckling. Unloads during the tests of the 16 and 60-inch wide panels in this study indicates that buckling was occurring even though anti-buckling guides were applied to the specimens. A finite element model is currently being developed that incorporates buckling effects. Once buckling effects are incorporated it may be possible to obtain good predictions with a constant value of A_p.

Prediction of Residual Strength for Two-Bay Crack

The experimental and predicted R-curves of 2024-T3 and C188-T3 from a 60-inch wide specimen were used to predict the residual strength of a two-bay crack in a representative fuselage structure (Figure 5). A common design policy is to ensure that structure can sustain a two-bay under the severest anticipated operating conditions. The crack was assumed to extend entirely across two bays ($2a_o$=40 inches) with the center stiffener (i.e., frame) failed. The stiffener material was assumed to be 7075-T6. The crack drive or K solution derived by Yeh (ref. 6) was used in the analysis. This solution is for a flat, stiffened panel subjected to uniform axial loading and does not include possible rivet or stiffener failure. It does account for shear deformation of the fasteners and bending deformation of the sheet and stiffeners.

RESULTS

Tensile Properties and Kahn Tear Results

The engineering stress-strain curves of the clad 2024-T3 and C188-T3 sheet are shown in Figure 6. True stress-strain curves were derived from these curves and used as inputs into the R-curve prediction method. The yield strength, ultimate tensile strength and total strain at failure are given in Table I. The tensile properties of the two alloys were nearly the same. The C188-T3 had a slightly higher yield strength and 2024-T3 had a slightly higher ultimate tensile strength. The total strain at failure was nearly identical in both materials.

The experimental and predicted Kahn tear test records are shown in Figure 7. The experimental responses of the 2024-T3 and C188-T3 were significantly different. The peak load and area under the curve of C188-T3 was greater than that of 2024-T3. The area under the load-displacement curve represents the energy required to fail the specimen.

Good agreement was obtained between the predicted and experimental Kahn tear test records. The values of J_i and A_p obtained from the finite element analysis are given in Table II. J_i was 34% greater and A_p 50% greater in C188-T3 than in 2024-T3 indicating the former had higher initiation toughness and better crack extension resistance. J_i is found to be primarily controlled by the peak load and A_p by the slope of the test record beyond peak load. The serrated appearance of the predicted test record after peak load is a consequence of discrete node release in the model.

Comparison of Experimental and Predicted R-curves

The experimental and predicted load-COD records and R-curves for the 6.3, 16 and 60-inch wide M(T) specimens are shown for 2024-T3 and C188-T3 in Figures 8, 9 and 10, respectively. The values

of J_i and A_p used in the predictions are given in Table II. Experimental and predicted R-curve data in Figures 8 through 10 are shown only up to the point where the net section stress in the uncracked specimen ligament based on physical crack length exceeds 100% of the material's yield strength. Experimental and predicted values of crack extension resistance, K_R, just prior to net section yielding are compared in Table III. The comparisons are at effective crack extensions of Δa_{eff}=0.4, 0.8, and 5 inches for the 6.3, 16, and 60-inch wide specimens, respectively.

The load-COD response of the 6.3-inch wide specimen was over predicted for both 2024-T3 and C188-T3 resulting in an over prediction of the R-curves (Figure 8). The difference between predicted and experimental K_R at Δa_{eff}=0.4 was 11% for the 2024-T3 and 4.4% for C188-T3. The agreement between experiment and prediction for C188-T3 was nearly perfect for the 16-inch wide specimen (Figure 9). The difference between predicted and experimental KR was less than 1%. There was no 16-inch wide specimen tested for 2024-T3. For the 60-inch wide specimen, the agreement between experiment and prediction for 2024-T3 was excellent, while the load-COD response and R-curve for C188-T3 were again over predicted (Figure 10). The difference between predicted and experimental K_R at Δa_{eff}=5 inches was 1.4% for 2024-T3 and 9.1% for C188-T3. Figure 10 also shows the R-curves from other lots of Alclad 2024-T3 and Alclad C188-T3 in the thickness range 0.036 to 0.249 inch. Comparison shows that the lots in this study are typical of production material.

Residual Strength Predictions for a Two-Bay Crack

The residual strength predictions for the representative fuselage structure obtained from the experimental and predicted R-curves from 60-inch wide panels are shown in Figure 11. The crack drive curves reflect a decrease in stress intensity factor as the crack approaches the intact stiffeners (i.e., frames). Failure occurs at the applied stress where the crack drive curve becomes tangent to the R-curve. This stress defines the maximum residual strength capacity of the structure with a two-bay crack. The residual strength prediction for the structure with Alclad 2024-T3 fuselage skin was 37 ksi using either the experimental or predicted R-curve. The prediction for a Alclad C188-T3 skin was 46 ksi using the experimental R-curve and 50 ksi using the predicted R-curve, a difference of 8%.

The extent of valid R-curve data from the 6.3 and 16-inch wide specimens are also shown in Figure 11. Beyond these values the 6.3 and 16-inch wide specimens exhibit net section yielding in violation of ASTM E561 validity requirements. Thus, the 6.3 and 16-inch wide specimen R-curves are clearly inadequate for predicting residual strength of the fuselage structure. The tangency point occurs at a much greater crack extension than can be obtained in these size panels. Residual strengths predicted from the predicted R-curves, while up to 8% higher than residual strengths predicted from the experimental R-curves obtained from 60-inch wide panels, are clearly more reliable than those that would be predicted using R-curves obtained from 6.3 or 16-inch wide specimens. The latter would significantly underestimate the residual strength of the structure.

DISCUSSION AND CONCLUSIONS

Experimental and predicted R-curves correlate reasonably well for the specimen geometries and alloys considered. The fact that reasonable R-curve predictions were obtained for a 60-inch wide M(T) specimen is especially encouraging, since R-curves from this size panel or larger are often needed to predict the fracture response of actual structural components. This was certainly the case for the two-bay crack in the representative fuselage structure in Figure 5.

The results indicate that the prediction method is a viable alternative to wide panel testing for material development and preliminary design. The problem of having insufficient R-curve for a residual strength prediction of a structural component is overcome by this method, since the finite element model can be adjusted to obtain an R-curve from any size wide panel specimen. The residual strength predictions for the two-bay crack in the fuselage structure using experimental and predicted R-curves were in reasonable agreement demonstrating the validity and usefulness of this method. However, it should be noted that none of the predictions were verified by testing actual structural components.

The method has several other advantages over wide-panel tests. The Kahn tear test is inexpensive, requires a minimal amount of material, and can be performed on almost any load frame. These are particularly advantageous in alloy development programs where there are a large number of variants and the amount of material for characterization is often limited. The prediction method will allow selection of alloys based on their predicted fracture behavior in intended structural applications, rather than on the basis of small-panel or toughness indicator results which may have little relevance to actual structural response. The Kahn tear test can also be performed in or after exposure to various environments or temperatures representative of service conditions. Testing of wide panels under these conditions may be impractical or prohibitively expensive.

However, additional work is needed to establish the generality of this approach and validate the method for a broader range of alloys and products. In particular, its applicability to thicker products needs to be explored. Since the R-curve is influenced by stress state, it is desirable to establish the validity of this approach over a full range of thickness encompassing plane stress to plane strain behavior. The sensitivity of the method to the input parameters (i.e., J_i, A_p, and stress-strain curve) also requires further investigation.

Both the experimental and predicted R-curves show the superior fracture toughness of C188-T3 sheet relative to 2024-T3. Residual strength calculations using the experimental R-curves indicate that the superior toughness yields a 24% higher load carrying capability for C188-T3 sheet in a representative fuselage structure.

ACKNOWLEDGMENTS

The authors would like to acknowledge the interest and encouragement provided by the Boeing Commercial Airplane Group. In particular we would like to thank Matt Miller, Sven Axter and Ken Barlow of Boeing for providing the 60-inch wide M(T) panel data and C188-T3 specimen remnants. The authors also thank fellow Alcoans Mark Mahler, Dick Rolf, Mike Kulak and Brian Cheney for their contribution to this effort.

REFERENCES

1. Macheret, J. and Yeh, J.R.: Aluminum R-Curve Estimated from Small Coupon Test Data. PDM Report No. 57-93-15, Alcoa Technical Center, Aluminum Company of America, 1993.

2. Luxmoore, A., Light, M.F. and Evans, W.T.: A Comparison of Energy Release Rates, the J-Integral and Crack Tip Displacements. *Int. J. Fracture,* vol.13, 1977, pp. 257-259.

3. Kobayashi, T., Irwin, G.R. and Zhang, X.J.: Topographic Examination of Fracture Surfaces in Fibrous-Cleavage Transition Behavior. *ASTM STP 827*, 1989, pp. 234-251.

4. Newman, J.C., Dawicke, D.S. and Bigelow, C.A: Finite-Element Analyses and Fracture Simulation in Thin-Sheet Aluminum Alloy. NASA TM-107662, 1992.

5. Kaufman, J.G. and Reedy, J.F.: Description and Procedure for Making Kahn-Type Tear Test. Alcoa Research Laboratories Report No. 9-M-681, Aluminum Company of America, 1966.

6. Yeh, J.R.: Fracture Analysis of a Stiffened Orthotropic Sheet. *Engineering Fracture Mechanics*, vol. 46, 1993, pp. 857-866.

Table I. Longitudinal Tensile Properties for 0.063-inch Alclad Sheet (1 lot each alloy)

Alloy	TYS (ksi)	UTS (ksi)	Total Strain at Failure (%)
2024-T3	50.7	66.0	17.6
C188-T3	52.6	64.8	17.3

Table II. Fracture Parameters for 0.063-inch Alclad Sheet (1 lot each alloy)

Alloy	Geometry	Fracture Parameter (L-T orientation)			
		J_i (ksi-in.)	A_p (in.^{2})*	F (kip)	F*A_p (kip-in.^{2})
2024-T3	Kahn Tear	0.35	8.00E-4	0.119	9.52E-5
	W=6.3 in. MT	0.35	7.87E-4	0.121	9.52E-5
	W=16 in. MT	0.35	7.21E-4	0.132	9.52E-5
	W=60 in. MT	0.35	6.14E-4	0.155	9.52E-5
C188-T3	Kahn Tear	0.47	1.20E-3	0.120	1.44E-4
	W=6.3 in. MT	0.47	1.18E-3	0.122	1.44E-4
	W=16 in. MT	0.47	1.08E-3	0.133	1.44E-4
	W=60 in. MT	0.47	9.23E-4	0.156	1.44E-4

* for d=0.2 inch

Table III. Comparison of Experimental and Predicted K_R at Discrete Δa_{eff} (1 lot each alloy)

MT Width (inch)	Δa_{eff} (inch)	Alclad 2024-T3 (0.063 in.)			Alclad C188-T3 (0.063 in.)		
		K_R, Exp (ksi$\sqrt{}$in.)	K_R, Pred (ksi$\sqrt{}$in.)	Δ%	K_R, Exp (ksi$\sqrt{}$in.)	K_R, Pred (ksi$\sqrt{}$in.)	Δ%
6.3	0.4	72.6	80.5	+11	81.4	85.0	+4.4
16	0.8	---	109.0	---	118.7	117.8	-0.8
60	5.0	188.4	185.6	-1.4	229.0	249.8	+9.1

Kahn Tear Test Model (J.R. Yeh, Y. Macheret)

Two Fracture Criteria:

J_i = Energy for Crack Initiation

A_p= Critical Crack-tip Opening Area for Propagation

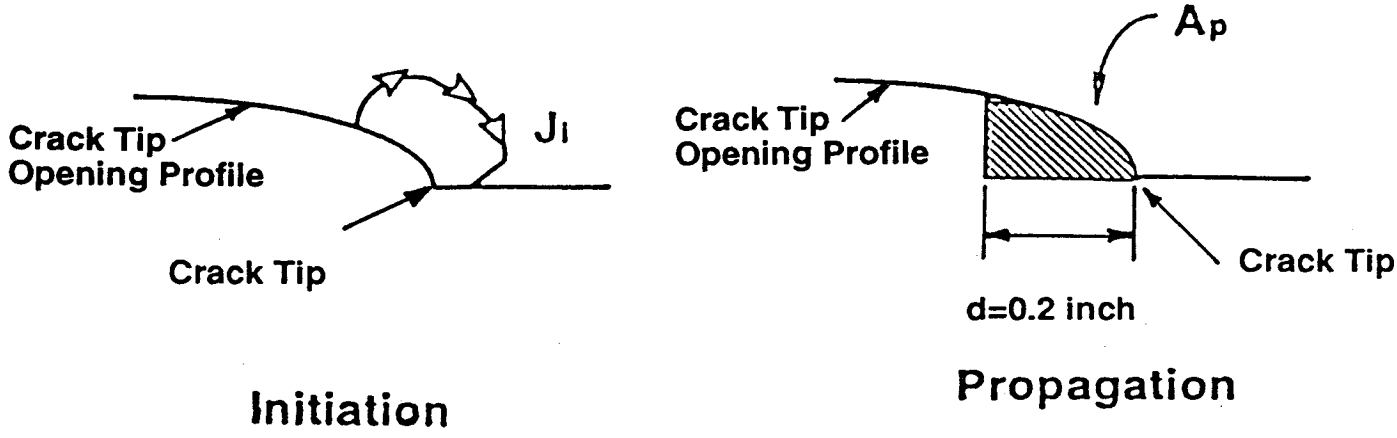

Figure 1. Fracture criteria used in R-curve prediction method.

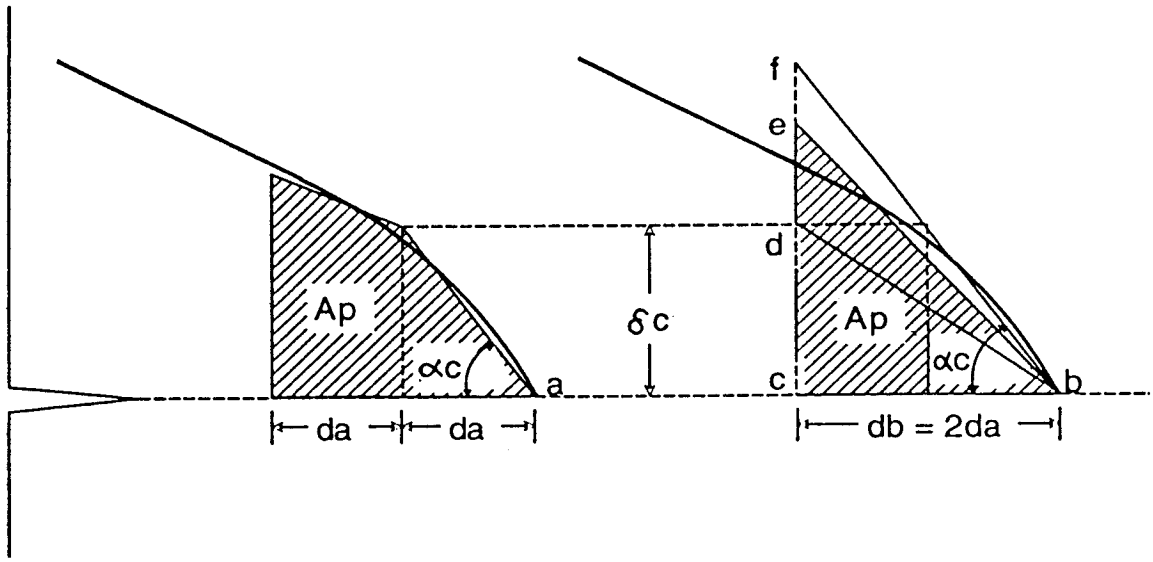

Figure 2. Schematic showing effect of element size for Ap, CTOA, and CTOD criteria.

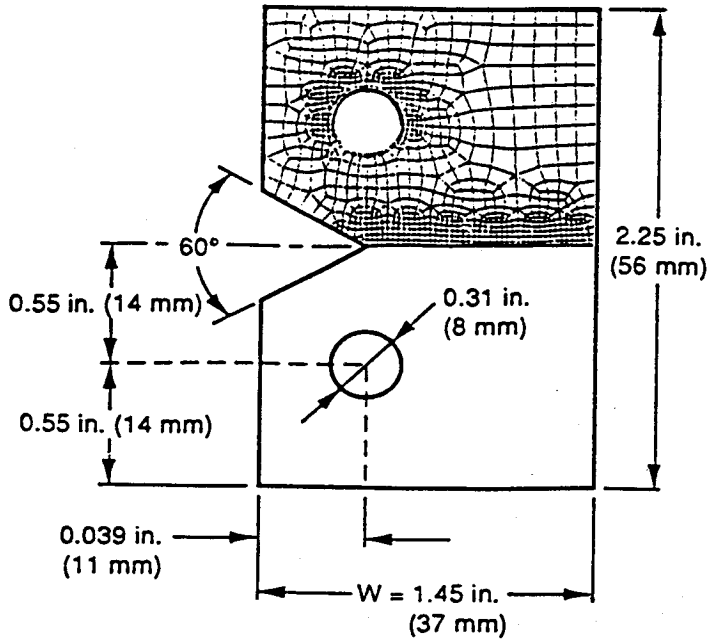

Figure 3. Kahn tear specimen and its finite element model.

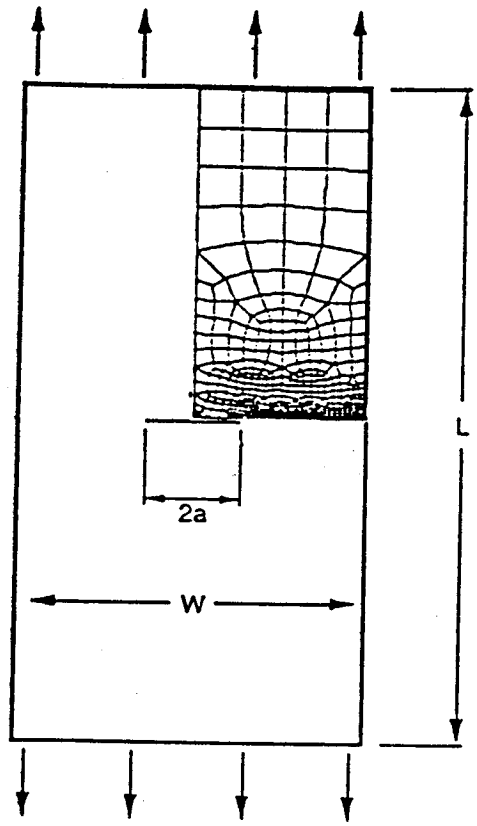

Figure 4. M(T) panel and its finite element model.

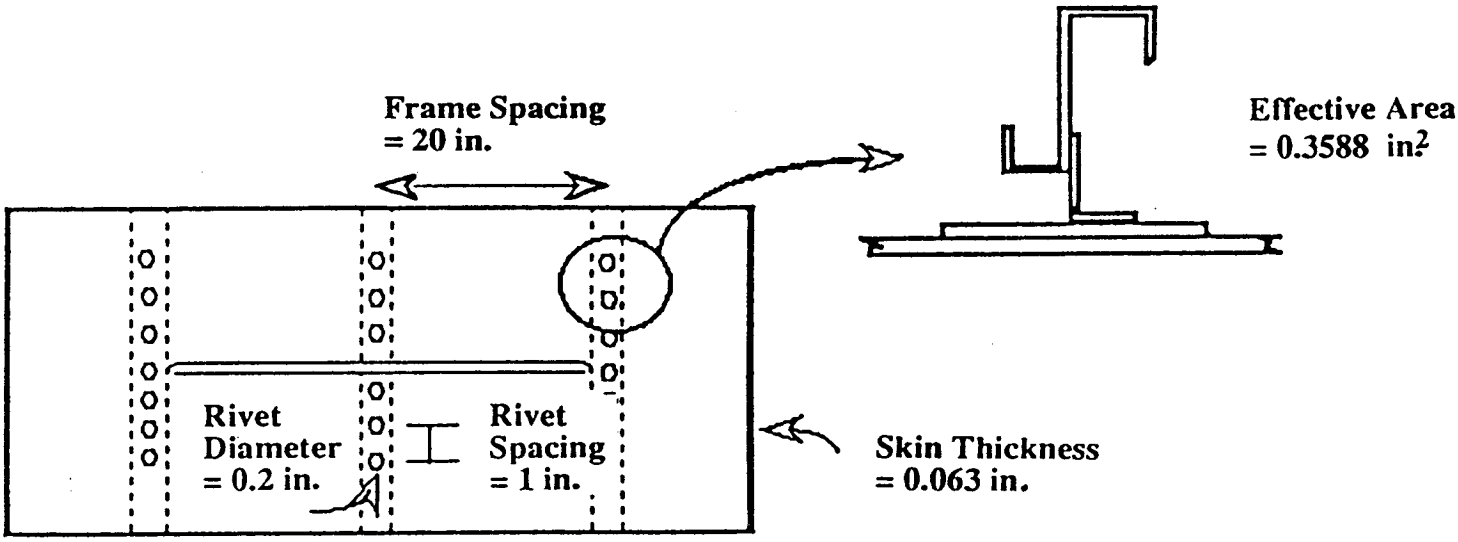

Figure 5. Representative fuselage structure with two-bay crack.

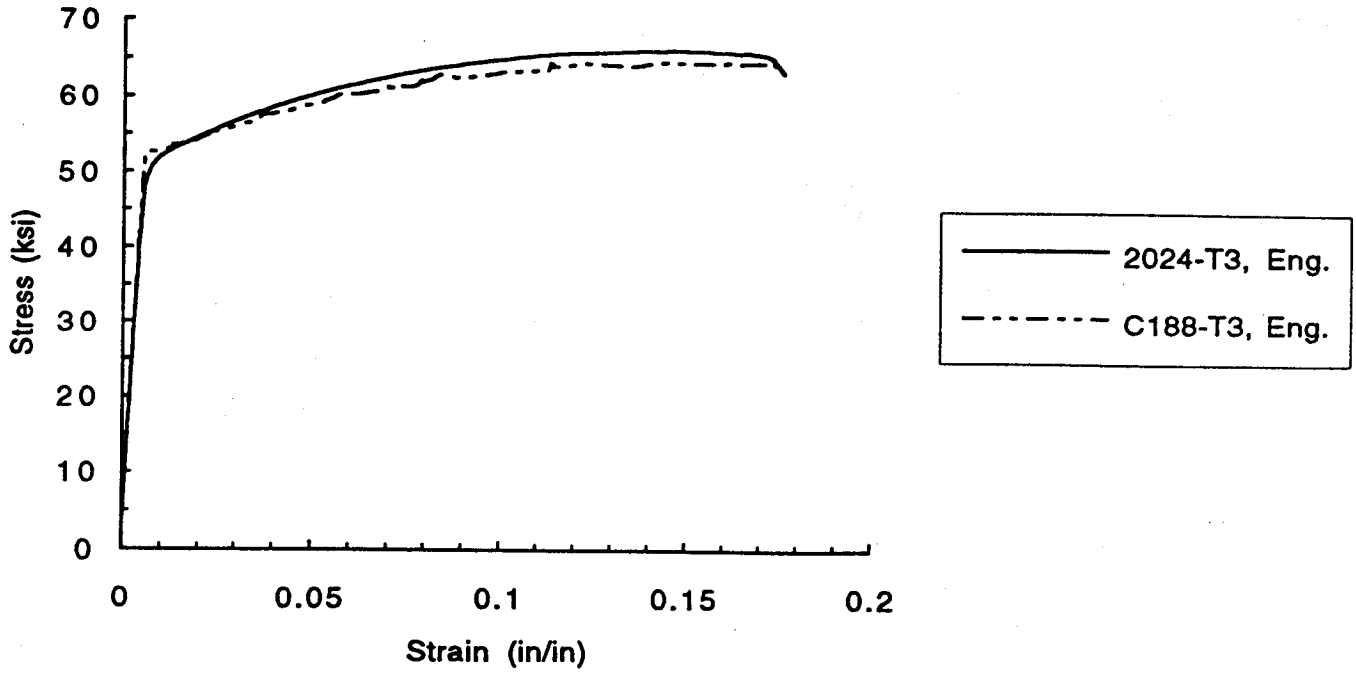

Figure 6. Engineering stress-strain curves for 0.063-inch Alclad 2024-T3 and Alclad C188-T3 sheet (1 lot each alloy).

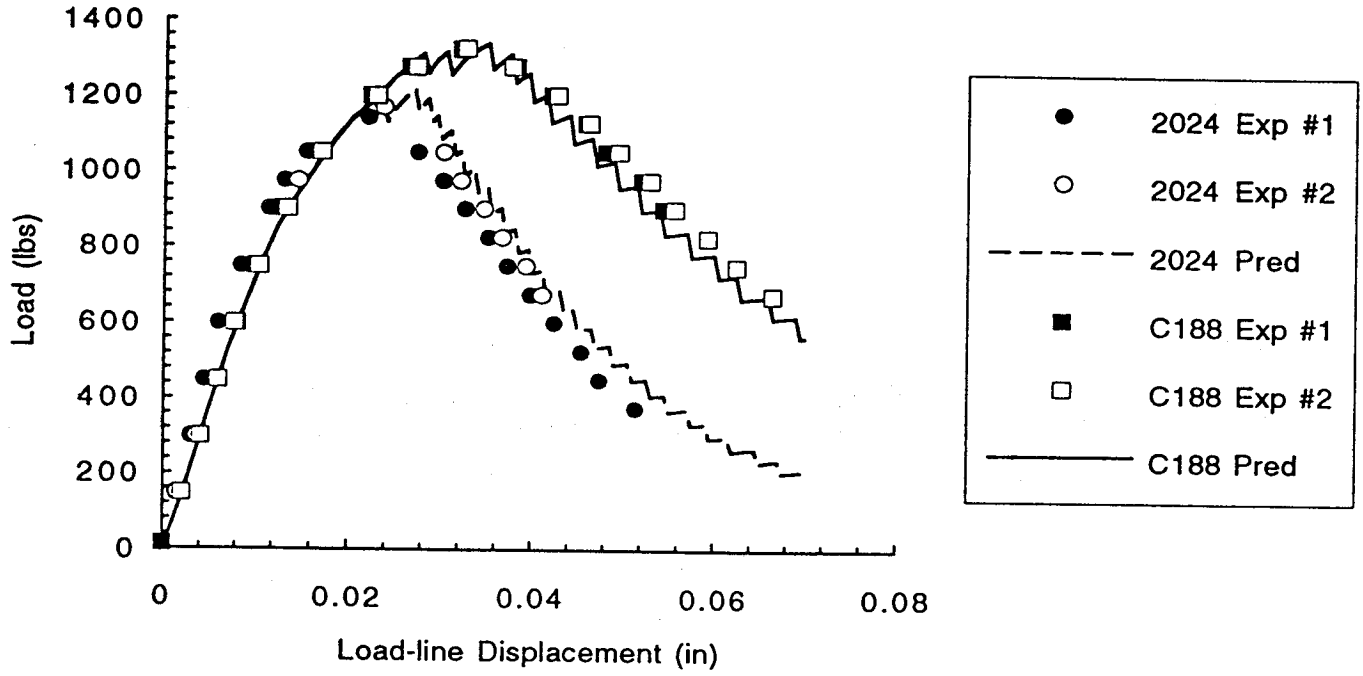

Figure 7. Predicted and experimental Kahn tear test records for Alclad 0.063-inch 2024-T3 and Alclad C188-T3 sheet (1 lot each alloy).

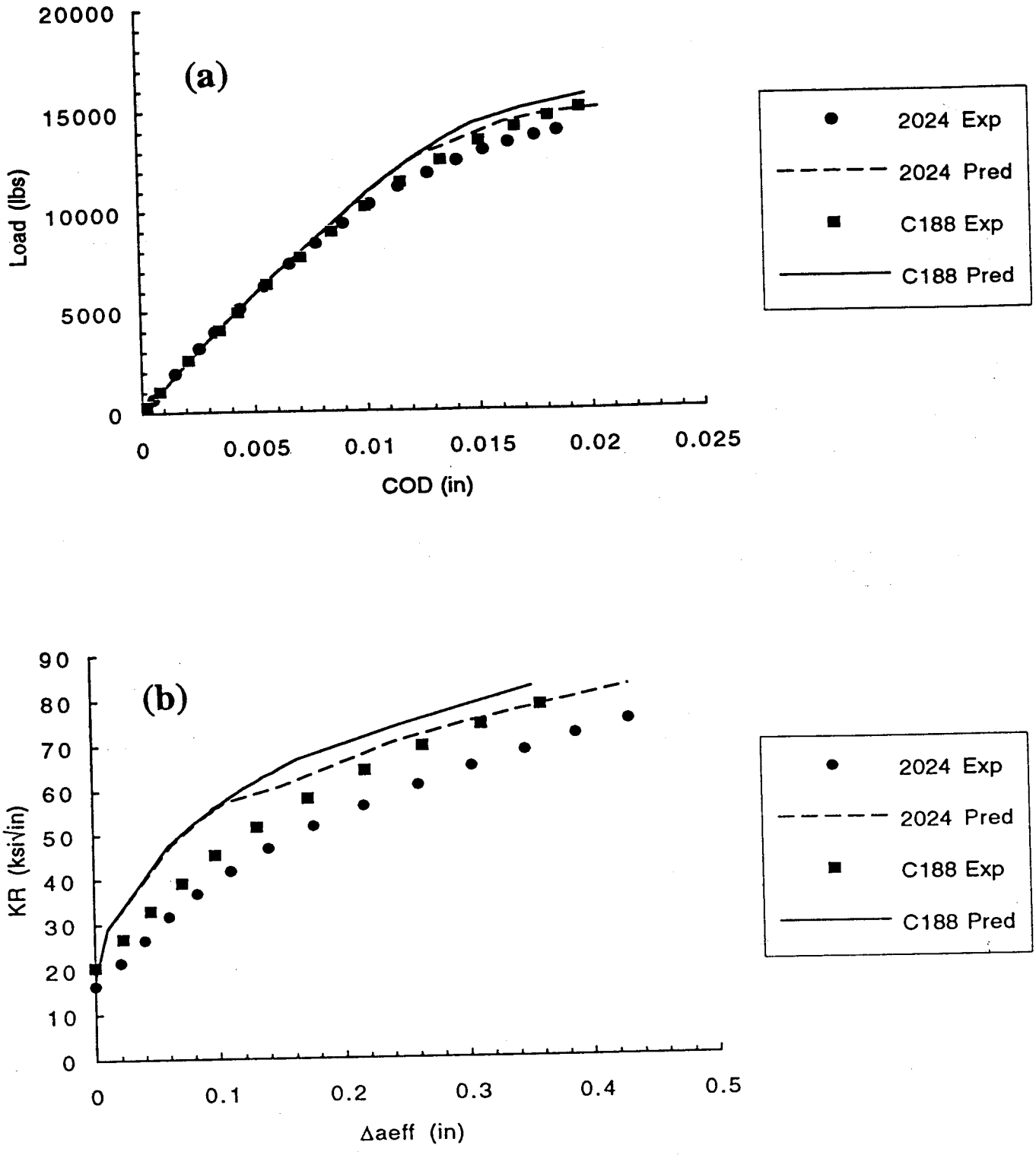

Figure 8. Predicted and experimental load-COD response (a) and R-curves (b) for 6.3-inch wide M(T) specimen.

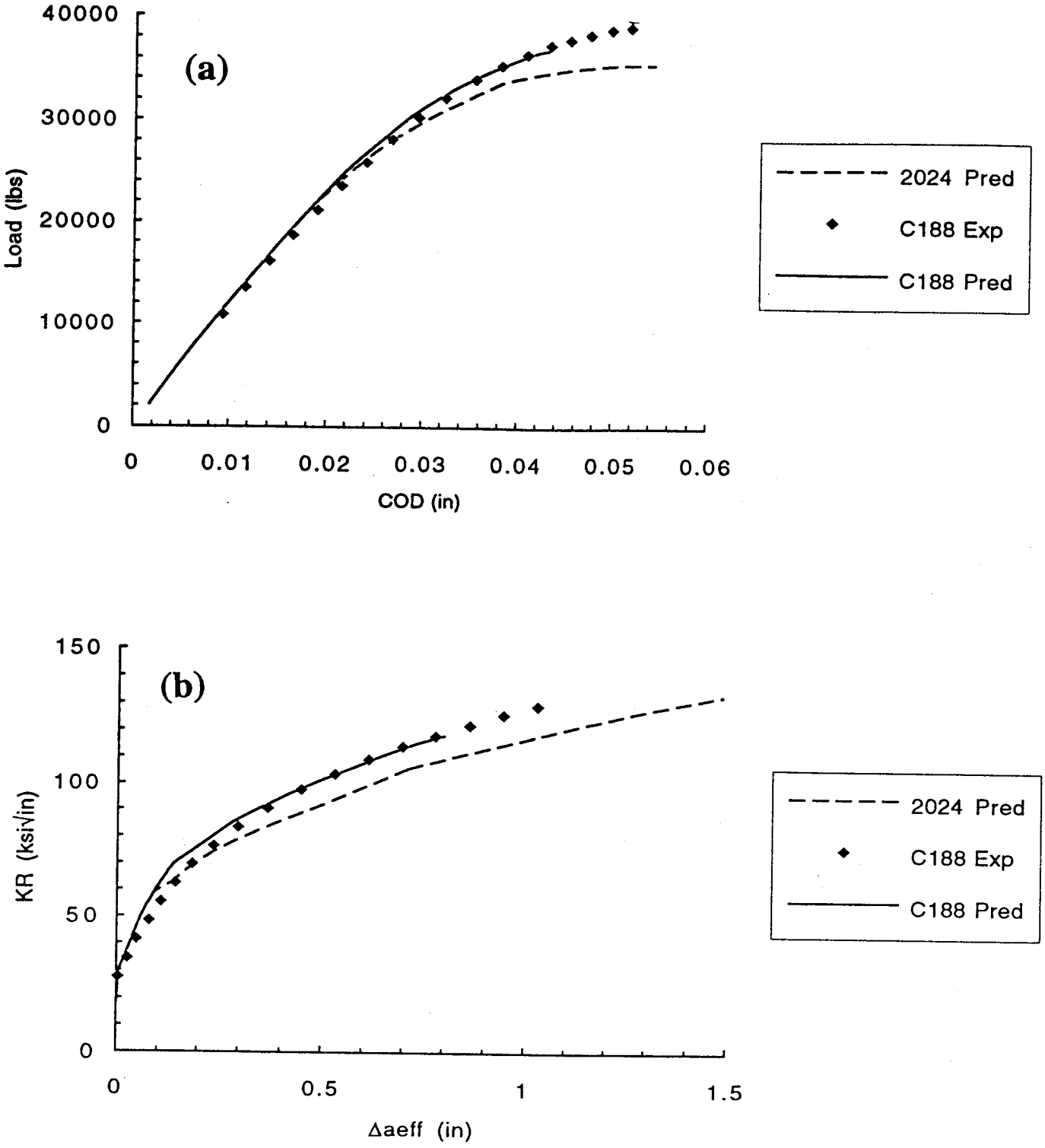

Figure 9. Predicted and experimental load-COD response (a) and R-curves (b) for 16-inch wide M(T) specimen.

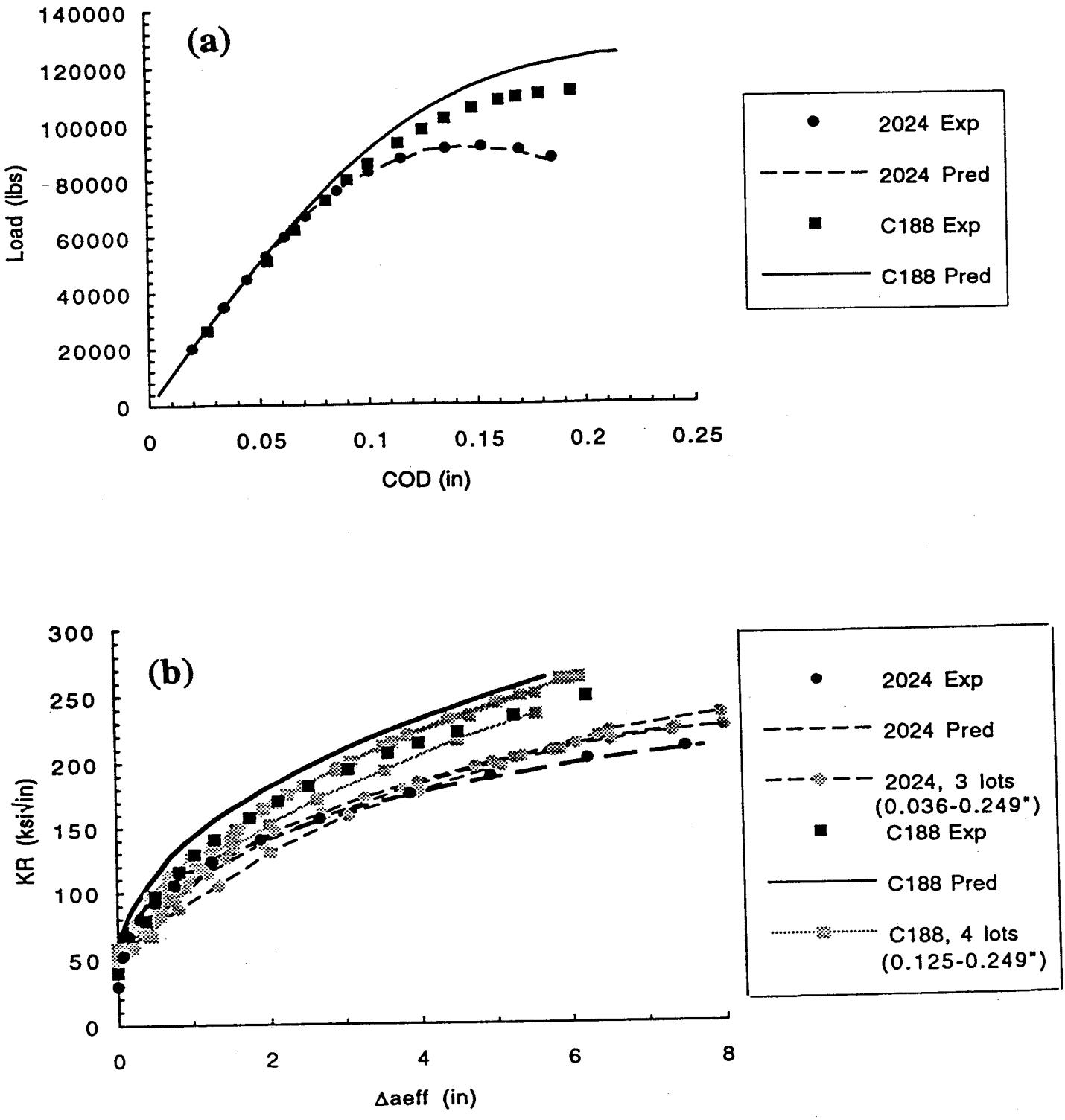

Figure 10. Predicted and experimental load-COD response (a) and R-curves (b) for 60-inch wide M(T) specimen

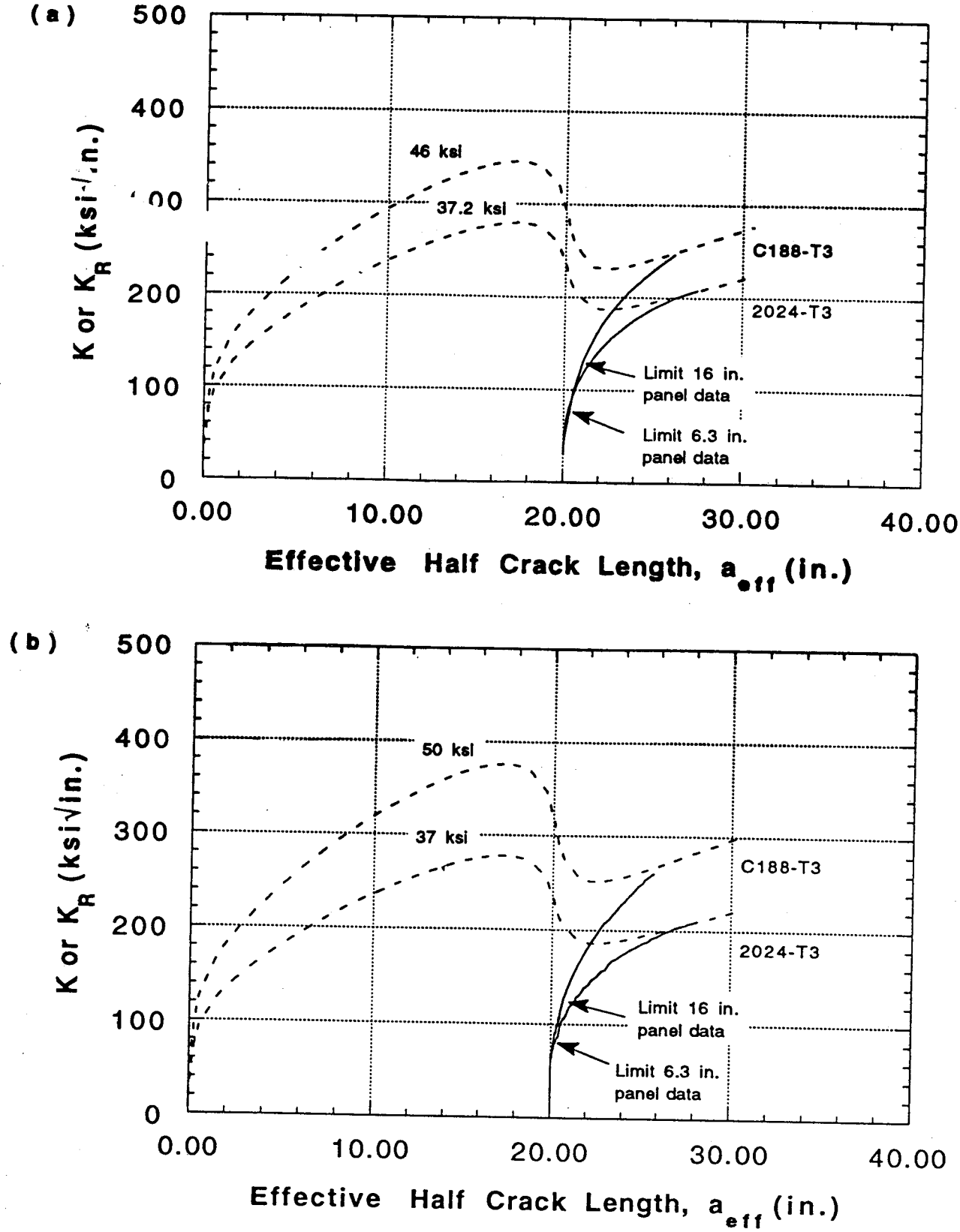

Figure 11. Residual strength prediction for two-bay crack in fuselage skin using experimental R-curves (a) and predicted R-curves (b) for Alclad 2024-T3 and Alclad C188-T3 0.063-inch sheet (1 lot each alloy).